Carbohydrate Polymers 93 (2013) 628–634

Contents lists available at SciVerse ScienceDirect

Carbohydrate Polymers

journal homepage: www.elsevier.com/locate/carbpol

Isolation and characterization of microcrystalline cellulose from oil palm biomass residue

M.K. Mohamad Haafiz[a,b], S.J. Eichhorn[c], Azman Hassan[a,*], M. Jawaid[d]

[a] Department of Polymer Engineering, Faculty of Chemical Engineering, Universiti Teknologi Malaysia, 81310 Skudai UTM, Johor, Malaysia
[b] School of Industrial Technology, Universiti Sains Malaysia, 11800 Penang, Malaysia
[c] College of Engineering, Maths & Physical Sciences, Physics Building, Stocker Rd, Exeter EX4 4QL, Devon, UK
[d] Laboratory of Biocomposite Technology, Institute of Tropical Forestry and Forest Products (INTROP), Universiti Putra Malaysia, 43400 UPM Serdang, Selangor, Malaysia

ARTICLE INFO

Article history:
Received 28 November 2012
Received in revised form
20 December 2012
Accepted 14 January 2013
Available online xxx

Keywords:
Oil palm empty fruit bunch
Pulp bleaching
Cellulose
Microcrystalline cellulose

ABSTRACT

In this work, we successfully isolated microcrystalline cellulose (MCC) from oil palm empty fruit bunch (OPEFB) fiber-total chlorine free (TCF) pulp using acid hydrolysis method. TCF pulp bleaching carried out using an oxygen–ozone–hydrogen peroxide bleaching sequence. Fourier transform infrared (FT-IR) spectroscopy indicates that acid hydrolysis does not affect the chemical structure of the cellulosic fragments. The morphology of the hydrolyzed MCC was investigated using scanning electron microscopy (SEM), showing a compact structure and a rough surface. Furthermore, atomic force microscopy (AFM) image of the surface indicates the presence of spherical features. X-ray diffraction (XRD) shows that the MCC produced is a cellulose-I polymorph, with 87% crystallinity. The MCC obtained from OPEFB-pulp is shown to have a good thermal stability. The potential for a range of applications such as green nano biocomposites reinforced with this form of MCC and pharmaceutical tableting material is discussed.

1. Introduction

Cellulose is a classical example of a renewable and biodegradable structural plant polymer which can be processed into whisker-like micro fibrils (Abraham et al., 2011; Eichhorn, 2011). Its remarkable reinforcing capability, excellent mechanical properties, low density and environmental benefits have drawn the attention of scientists to utilize cellulose to develop environmentally friendly polymer composites or green composites (Eichhorn et al., 2010). Cellulose is the world's most ubiquitous and abundant natural occurring polymer which is produced by plants, as well as by microorganism (Klemm, Heublein, Fink, & Bohn, 2005). It is a linear homopolymer of glucose $(C_6H_{10}O_5)_n$ with repeating units consisting of D-glucose in a $^4C_1$ conformation, which is insoluble in water but degradable by microbial and fungal enzymes (Li et al., 2009). In nature, the cellulose molecular chains are biosynthesized and self-assembled into microfibrils, which are composed of crystalline and amorphous domains (Fernandes et al., 2011; Nishiyama, 2009).

These aggregated cellulose molecules are stabilized laterally by hydrogen bonds between the hydroxyl groups and oxygens of adjacent molecules (Nishiyama, 2009). The amorphous regions of native cellulose can be readily hydrolyzed, with almost no weight loss, when subjected to strong acid hydrolysis (Rånby, 1951). Typically when wood sources are used the particles of hydrolyzed cellulose obtained are ~100–300 nm in length and ~3–10 nm in width. These nanoparticles are referred to as "nanocrystalline cellulose" or "microcrystalline cellulose" despite their nano scale dimension (Bras et al., 2010; De Menezes, Siqueira, Curvelo, & Dufresne, 2009; Goetz, Mathew, Oksman, Gatenholm, & Ragauskas, 2009).

Microcrystalline cellulose (MCC) is a fine, white, odorless, crystalline powder, and a biodegradable material, which can be isolated from cellulose and used as a suspension stabilizer and a water-retainer, in the cosmetics, food, and pharmaceuticals industries (Chuayjuljit, Su-uthai, & Charuchinda, 2010; El-Sakhawy & Hassan, 2007). Industrial scale MCC is obtained through hydrolysis of wood and cotton cellulose by using dilute mineral acids. MCC is typically characterized by a high degree of crystallinity, although there are variations between grades; values typically range from 55 to 80% as determined by X-ray diffraction (XRD) (Chuayjuljit et al., 2010). Cellulose obtained from different origins and hydrolysis conditions differ in crystallinity, moisture content, surface area, porous structure, particle size and molecular weight (De Menezes et al., 2009; El-Sakhawy & Hassan, 2007; Li et al., 2009).

Recently researchers reported the extraction of cellulose fibers from rice husk by alkali and bleaching treatments, which were subsequently converted to nanocrystals using a sulfuric acid (H_2SO_4) hydrolysis treatment (Johar, Ahmad, & Dufresne, 2012). Isolation of microcrystalline cellulose has been carried out from jute cellulose by using the same acid hydrolysis (H_2SO_4) approach

* Corresponding author. Tel.: +60 7 5537835; fax: +60 7 5581 463.
E-mail address: azmanh@cheme.utm.my (A. Hassan).

0144-8617/$ – see front matter © 2013 Elsevier Ltd. All rights reserved.
http://dx.doi.org/10.1016/j.carbpol.2013.01.035

(Jahan, Saeed, He, & Ni, 2011). Researchers have also produced cellulose nanofibers by hydrolyzing oil palm empty fruit bunch fibers (Fahma, Iwamoto, Hori, Iwata, & Takemura, 2010). In addition to these isolation studies, the synthesis and characterization of cellulose phosphate from oil palm empty fruit bunch derived microcrystalline cellulose has been reported (Wanrosli, Rohaizu, & Ghazali, 2011; Wanrosli, Mohamad Haafiz, & Azman, 2011b).

In recent years, there has been enormous interest in producing nanocomposite materials. This interest is due to the extraordinary properties exhibited as a result of the nanoscale reinforcement which offers properties such as high surface area for bonding with resins, optical transparency and additional/multifunctional properties, e.g. electrical conduction. In order to produce fully renewable and biodegradable nanocomposites, both the polymer matrix and the nano reinforcement have to be derived from renewable resources (Azizi Samir, Alloin, & Dufresne, 2005; Petersson, Kvien, & Oksman, 2007). MCC has attracted the attention of researchers to use it as a potential starting material for cellulose reinforced nanocomposites (Mathew, Oksman, & Sain, 2005). It also reported that the origin of raw materials and method of preparation influences the overall characteristics of MCC (Lee et al., 2009). They also reported that MCC can be used as universal filler for the extrusion/spheronization process. Cellulose nanofibers display exceptional mechanical properties, such as high modulus (~140 GPa; Sturcova, Davies, & Eichhorn, 2005). They are also ideal materials to use as reinforcement in a transparent polymeric matrix because they are free from light scattering. This is due to their lateral dimensions being smaller than the wavelength of visible light, e.g. bacterial cellulose fibrils (Yano et al., 2005).

The isolation and characterization of MCC from OPEFB has previously been reported, but until now no researchers have reported a comprehensive characterization of isolated MCC from OPEFB, or its comparison with OPEFB-pulp and commercial MCC.

2. Experimental

2.1. Materials

Fibrous strands of OPEFB were supplied by Sabutek (Malaysia), Teluk Intan, Perak. OPEFB-MCC was obtained from total chlorine free (TCF) pulping and bleaching of OPEFB-pulp, as described by Leh, Wanrosli, Zainuddin, and Tanaka (2008); this method is based on the procedures described by Wanrosli, Leh, Zainuddin, and Tanaka (2003). The chemical used for extracting OPEFB-MCC was ammonium hydroxide (NH_4OH) and hydrochloric acid (HCl) 32%, purchased from Merck, Malaysia. Commercially available MCC, Avicel® PH 101, Fluka, supplied by Sigma Aldrich, USA, with a size of ~50 μm, was used as reference which is denoted as C-MCC.

2.2. Methods

2.2.1. Preparation of microcrystalline cellulose

MCC was isolated from OPEFB-pulp using same method described by Chuayjuljit et al. (2010) based on original procedures described by Battista (1950). OPEFB-pulp was hydrolyzed with 2.5 N HCl at 105 °C ± 2 °C for 30 min with constant agitation in the ratio of 1:20 pulp over liquor. The reaction mixture was then filtered at room temperature, and washed repeatedly with distilled water. Following this 5% diluted NH_4OH was used to wash the mixture. Finally, distilled water was used to rinse the mixture until it was free from acid. The MCC obtained from OPEFB-pulp was then dried in a vacuum oven at 105 °C until constant weight was achieved. The resultant MCC was ground into a fine powder by using rotary ball mill. The OPEFB-MCC after washing and drying was snowy-white in appearance.

3. Characterization

3.1. Fourier transform infrared spectroscopy

Fourier transform infrared spectroscopy (FT-IR) was performed on a Perkin Elmer 1600 infrared spectrometer using the KBr method in the ratio of 1:100 and made to a pellet. FT-IR spectra of the coated pellet were recorded by using a Nicolet AVATAR 360 at 32 scans with a resolution of 4 cm^{-1} and within the wave number range of 370–4000 cm^{-1}. The positions of significant transmittance peaks were determined by using the "find peak tool" provided by the Nicolet OMNIC 5.01 software.

3.2. Morphological analysis

The morphology and size distribution of samples were studied by using SEM and AFM. SEM was carried out using a SEM-EDX Oxford INCA 400 model at an acceleration voltage of 15 kV. The samples were sputter-coated with gold to avoid charging. AFM measurements were performed using SPA-300HV atomic force microscope with an SPI 3800 controller. A dilute drop of cellulose suspension was dispersed on the surface of an optical glass slide and allowed to dry at room temperature prior to analysis.

3.3. X-ray diffraction

X-ray diffraction (XRD) was carried out to study the crystallinity of the samples using an X'Pert X-ray diffractometer (SIEMENS XRD D5000) and Ni-fltered Cu Kα radiation at an angular incidence of 10–60° (2θ angle range). The operating voltage and current were 40 kV and 50 mA, respectively. The crystallinity of the samples was calculated from diffraction intensity data using the empirical method for native cellulose (Rosa, Rehman, De Miranda, Nachtigall, & Bica, 2012). The crystalline-to-amorphous ratio of materials was determined using Eq. (1).

$$C_r.I(\%) = \frac{I_{002} - I_{am}}{I_{002}} \quad (1)$$

where *Cr.I* is the crystallinity index, I_{002} is the maximum intensity (in arbitrary units) of the diffraction from the 002 plane at $2\theta = 22.6°$, and I_{am} is the intensity of the background scatter measured at $2\theta = 19°$.

3.4. Thermogravimetric analysis (TGA)

The thermal stability of samples was characterized using a thermogravimetric analyzer, model 2050 (TA Instruments, New Castle, DE). The specimens were scanned from 30 °C to 900 °C at a rate of 20 °C min^{-1} under a nitrogen gas atmosphere.

4. Results and discussion

4.1. FT-IR analysis

Typical FT-IR spectra of OPEFB-pulp, OPEFB-MCC and C-MCC are shown in Fig. 1. The vibrational assignments are summarized in Table 1. All samples display two main absorbance regions as reported by Rosa et al. (2012) and Fahma et al. (2010). These regions are found at high wavenumbers (2800–3500 cm^{-1}) and low wavenumbers (500–1700 cm^{-1}), respectively. FT-IR spectroscopy revealed the similarities between all spectra which is an indication that all samples have similar chemical compositions. Comparable results have been obtained by Wanrosli, Rohaizu, et al., 2011, who compared OPEFB-MCC with pure cellulose before regeneration into cellulose phosphate. Another study also obtained similar results

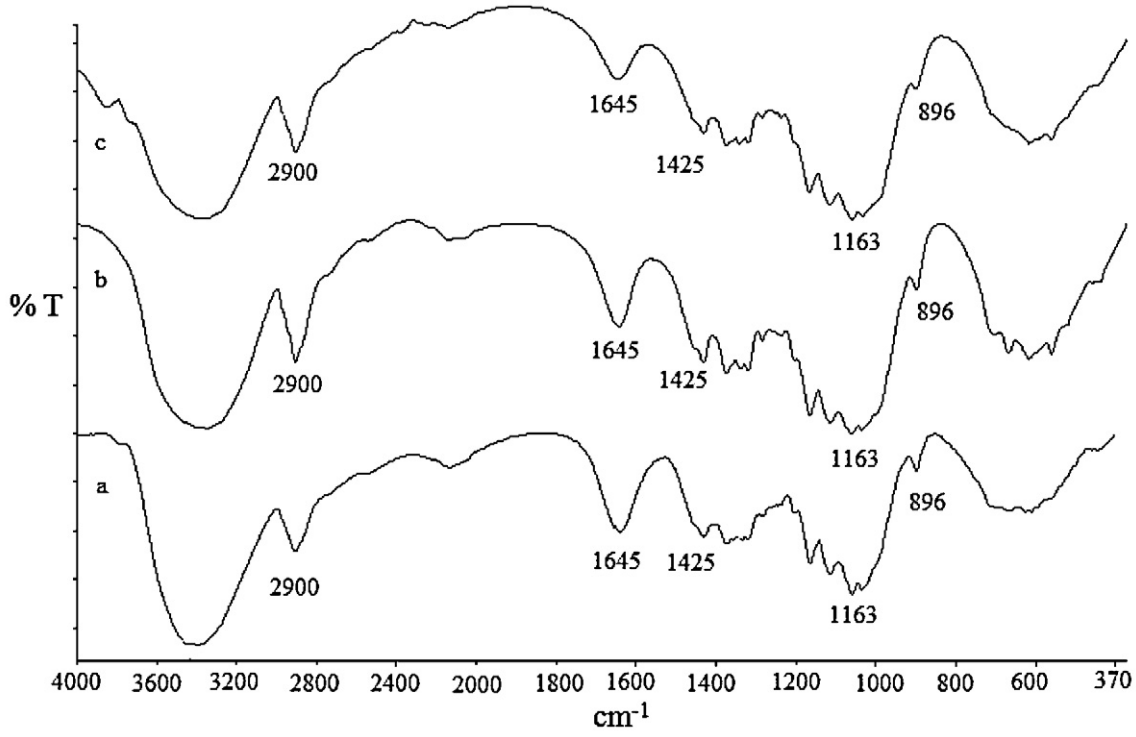

Fig. 1. Typical FT-IR spectra obtained from (a) OPEFB-pulp, (b) OPEFB-MCC, and (c) C-MCC.

while producing the MCC from OPEFB holocellulose as a starting material (Rosnah, Astimar, Wan Hasamudin, & Gapor, 2009). Fahma et al. (2010) also reported the same result when isolating nanofibers from OPEFB by using different concentrations of sulfuric acid (H_2SO_4).

The broad absorption band located from 3400 to 3500 cm^{-1} is due to stretching of –OH groups and an absorption at 2900 cm^{-1} is related to CH_2 groups (Jahan et al., 2011; Rosa et al., 2012; Satyamurthy, Jain, Balasubramanya, & Vigneshwaran, 2011). The absorption at 1645 cm^{-1} in all samples is indicative of absorption of water. According to other studies, this band is related to the bending modes of water molecules due to a strong interaction between cellulose and water (Johar et al., 2012; Rosa et al., 2012). The absorption band at 1425 cm^{-1} is associated to the intermolecular hydrogen at the C_6 (aromatic ring) group (Kumar, Maria De La, & Yang, 2002). The absorption band at 1163 cm^{-1} corresponds to C—O—C stretching, and the peak at 896 cm^{-1} is associated to C—H rock vibration of cellulose (anomeric vibration, specific for β-glucosides) observed in OPEFB-pulp, OPEFB-MCC, and C-MCC samples (Alemdar & Sain, 2008a; Fahma et al., 2010; Li et al., 2009).

According to previous work the absence of peaks located in the range 1509–1609 cm^{-1}, which would correspond to C=C aromatic skeletal vibrations, indicate the complete removal of lignin (Fahma et al., 2010; Rosa et al., 2012). The absorption band which corresponds to either the acetyl or uronic ester groups of hemicelluloses normally appears in the region 1700–1740 cm^{-1}, this band is absent, indicating the removal of hemicelluloses (Alemdar & Sain, 2008a; Nuruddin et al., 2011; Rosa et al., 2012). Similar results have been observed by Jahan et al. (2011) during production of MCC from jute fibers and Fahma et al. (2010) also reported similar results when isolating nanofibers from OPEFB.

The FT-IR spectra show that the acid hydrolysis reaction performed to obtain OPEFB-MCC from OPEFB-pulp does not affect the chemical structure of the cellulosic fragments. It mean that acid hydrolysis of OPEFB-pulp did not affect the cellulosic components of OPEFB-MCC. Their surface morphologies may however be affected.

Table 1
FTIR spectral peak assignments for OPEFB-pulp, OPEFB-MCC and C-MCC.

Peak frequency (cm^{-1}) for OPEFB-pulp, OPEFB-MCC, and C-MCC	Peak assignment
3400–3500	OH-bending
2800–2900	CH_2 groups
1645	O—H stretching
1425	CH_2 bending
1163	C—O—C stretching
896–900	C—H

4.2. Morphological analysis

The morphology of OPEFB-pulp and OPEFB-MCC after acid hydrolysis was investigated using SEM and compared to C-MCC. Scanning electron micrographs show changes in the morphology of the fibers in terms of size and level of smoothness after acid hydrolysis. It is however worth noting, as seen in Fig. 2, that acid hydrolysis altered the morphology of OPEFB-MCC compared to OPEFB-pulp. Fig. 2(a) shows individualized and uniform fibers, which correlates with the spectroscopic evidence for the removal of cementing material around the fiber bundles; namely hemicelluloses, and lignin (Alemdar & Sain, 2008a; Johar et al., 2012). OPEFB-pulp also showed a smooth fiber surface. Meanwhile, Fig. 2(b) shows irregular shaped fibrils, which are often aggregated, and a rough surface morphology. According to Mathew, Oksman, and Sain (2006), the roughness of MCC favors the production of nanocrystals *via* hydrolysis. Similar morphologies have been observed during isolation of MCC from OPEFB α-cellulose (Rosnah et al., 2009). C-MCC shows a similar morphological topography as compared to OPEFB-MCC (Fig. 2c), although much larger aggregates are present, with presumably lower aspect ratios. According to previous studies, cellulose obtained from different sources and

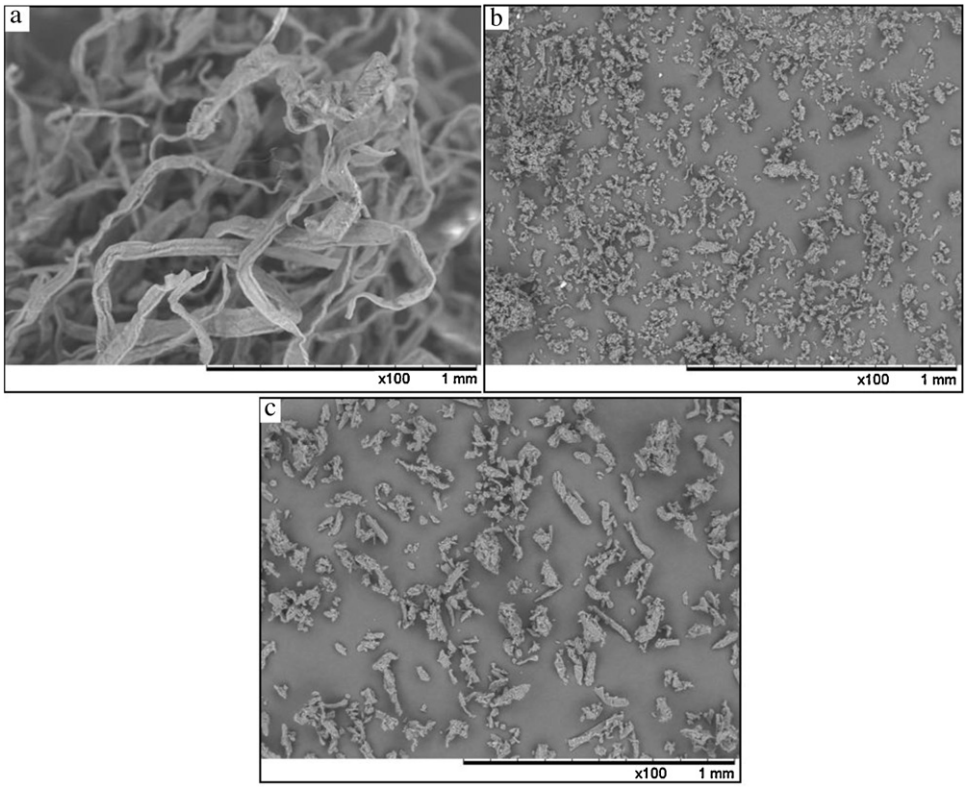

Fig. 2. Typical scanning electron micrographs of (a) OPEFB-pulp, (b) OPEFB-MCC, and (c) C-MCC.

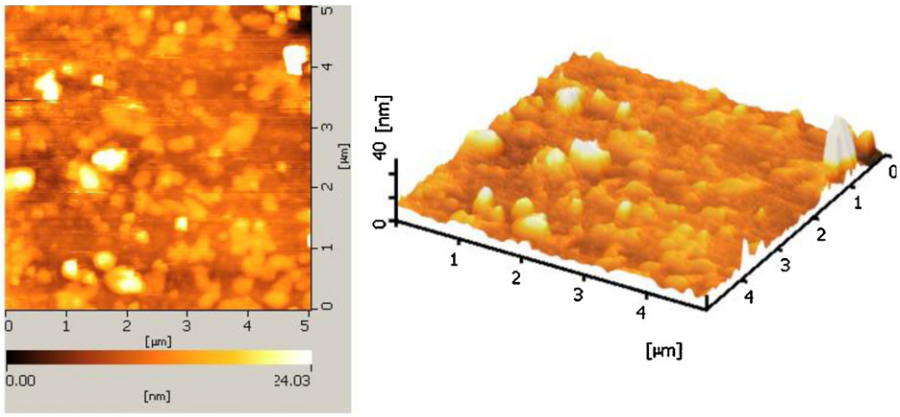

Fig. 3. Typical atomic force microscope images of OPEFB-MCC, height view (left) and 3D view (right).

hydrolysis conditions differ in overall characteristics of MCC such as particle size and aggregation (De Menezes et al., 2009; Lee et al., 2009). Typical AFM images of OPEFB-MCC are shown in Fig. 3. The three-dimensional image in Fig. 3 reveals that OPEFB-MCC show regular spherical particles and surface roughness due to highly aggregated OPEFB-MCC.

4.3. X-ray diffraction

It is widely recognized that cellulose contains both crystalline and amorphous region (Klemm et al., 2005). The X-ray diffraction (XRD) patterns of OPEFB-pulp, OPEFB-MCC, and C-MCC are presented in Fig. 4(a)–(c). The crystallinity of each sample is listed in Table 2. The crystallinity values of OPEFB-pulp and OPEFB-MCC were 80% and 87%, compared to C-MCC, which exhibited 79% crystallinity. All XRD diffraction data suggested the samples were highly crystalline native cellulose I, with no cellulose II present; indicated by the absence of the doublet located at 22.6° (Rosa et al., 2012; Satyamurthy et al., 2011). Our results are different to those obtained from MCC derived from OPEFB-α-cellulose, which show presence of small percentage of cellulose II by the presence of the doublet peak (Rosnah et al., 2009).

From Fig. 4(b) it is clear that the diffraction peak located at 22.6° becomes sharper, indicating an increase in crystallinity. An increase in the crystallinity is related to increases in the

Table 2
Crystallinity of OPEFB-pulp, OPEFB-MCC and C-MCC.

Sample	Crystallinity %
OPEFB-pulp	80
OPEFB-MCC	87
C-MCC	79

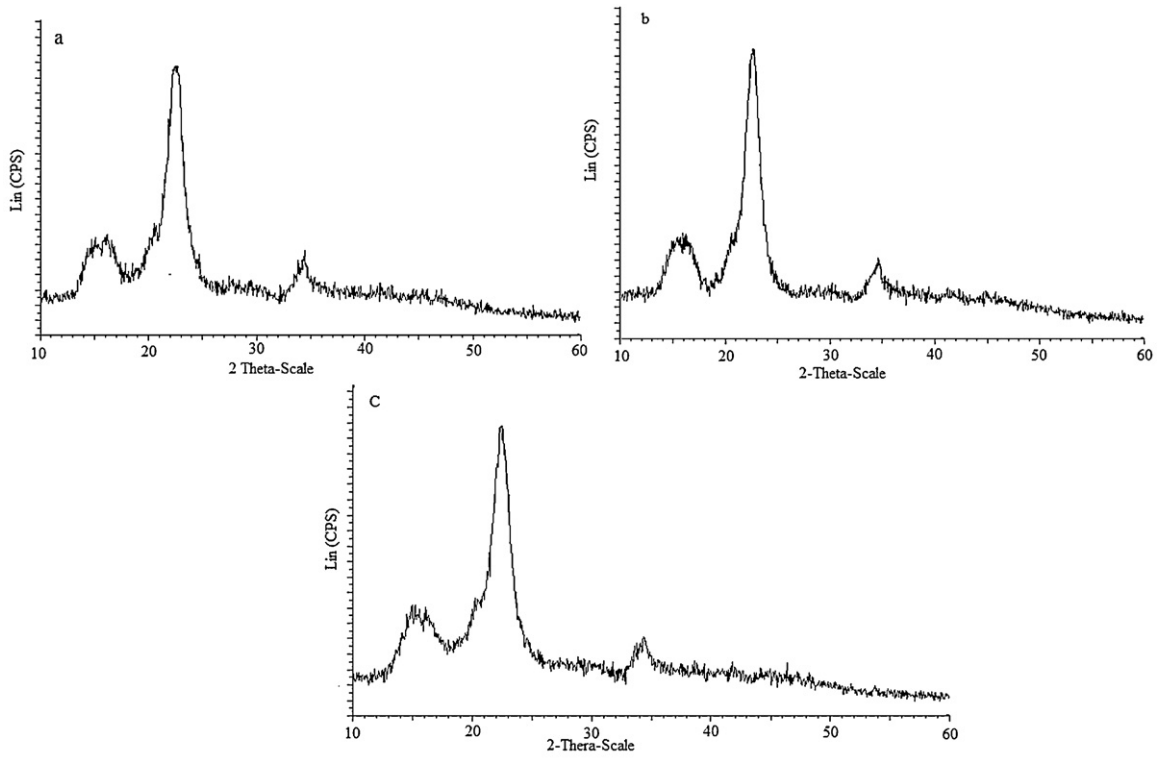

Fig. 4. X-ray diffractograms from (a) OPEFB-pulp, (b) OPEFB-MCC, and (c) C-MCC.

rigidity of the cellulose structure, which can lead to a higher tensile strength to fibers. This increase would be expected to increase the mechanical properties of composites (Alemdar & Sain, 2008b; Rosa et al., 2012). The crystallinity index for OPEFB-pulp is high due to removal of hemicellulsoe and lignin, which existed in amorphous regions leading to realignment of cellulose molecules (Li et al., 2009). The highest crystallinity index obtained for OPEFB-MCC is thought to be due to the removal of the amorphous regions of cellulose by acid hydrolysis, which prompts the hydrolytic cleavage of glycosidic bonds, finally releasing individual crystallites (Li et al., 2009; Spagnola et al., 2012). MCC produced from OPEFB-pulp in our study displays a higher crystallinity compared to nanocellulose produced from OPEFB by a chemo-mechanical technique (69%) (Jonoobi, Khazaeian, Md Tahir, Azry, & Oksman, 2011). Fahma et al. (2010) produced nanofibers from OPEFB by using H_2SO_4, and reported ~59% crystallinity. Jahan et al. (2011) also isolated MCC from jute by using H_2SO_4 and obtained an MCC with ~75% crystallinity.

4.4. Thermogravimetric analysis

Investigating the thermal properties of reinforcing materials is important in order to know their applicability for biocomposite processing at high temperatures (Alemdar & Sain, 2008b). Fig. 5 reports thermogravimetric analysis (TGA), and derivative thermogram (DTG) curves for OPEFB-pulp and OPEFB-MCC. Thermal degradation of OPEFB-pulp and OPEFB-MCC gave an initial weight loss in the range of 50–180 °C due to the evaporation of loosely bound moisture on the surface of the samples (Das et al., 2009; Li et al., 2009; Rosa et al., 2012). OPEFB-pulp and OPEFB-MCC samples show two-step degradation. The OPEFB-pulp and OPEFB-MCC started to decompose at 300 °C and 275 °C, respectively, which are higher temperatures compared to the thermal degradation of nanofibers produced from OPEFB fibers (Fahma et al., 2010). The thermal degradation data of OPEFB-pulp and OPEFB-MCC are tabulated in Table 3, using the temperatures at which 10% weight loss of the samples occurs and the residual weight at 400 °C, donated as the char residue.

The onset decomposition temperature and the temperature at which 10% degradation occurred for OPEFB-pulp were higher than for OPEFB-MCC. From Fig. 5, the decomposition temperatures peak for both samples can be seen in the derivative weight loss curve. These temperatures were designated as T_{max}, and are summarized in Table 3. The major decomposition peak temperature of OPEFB-MCC is observed at 326 °C while for OPEFB-pulp this occurs at 371 °C; these temperatures are where cellulose degrades. According to Jonoobi et al. (2011) cellulosic materials degrade at low to moderate temperatures. Early decomposition of hemicelluloses begins below 400 °C followed by pyrolysis of lignin, depolymerization of cellulose, active flaming combustion and char oxidation.

The higher decomposition temperature ($T_{10\%}$ and T_{max}) of OPEFB-pulp compared to OPEFB-MCC is thought to be due to a drastic reduction in molecular weight of the latter because of hydrolysis which makes it more susceptible to degrade when temperature increases. It is also believed that hydrolysis of cellulose not only dissolves the amorphous regions, but also some crystalline regions (Mandal & Chakrabarty, 2011). Similar results have been reported by El-Sakhawy and Hassan (2007) when producing MCC from baggase fibers. However, it is interesting to note that at 400 °C the weight loss for OPEFB-pulp is 88% compared to that of OPEFB-MCC (80%). Further heating showed that from 400 °C to 900 °C the

Table 3
Thermal properties of OPEFB-pulp and OPEFB-MCC.

Samples	Degradation temp (°C) $T_{10\%}$	Residual weight % at 400 °C	DTG peak temp (°C) T_{max}
OPEFB-MCC	293	20	326
OPEFB-pulp	308	12	371

$T_{10\%}$: Temperatures at which 10% weight loss.

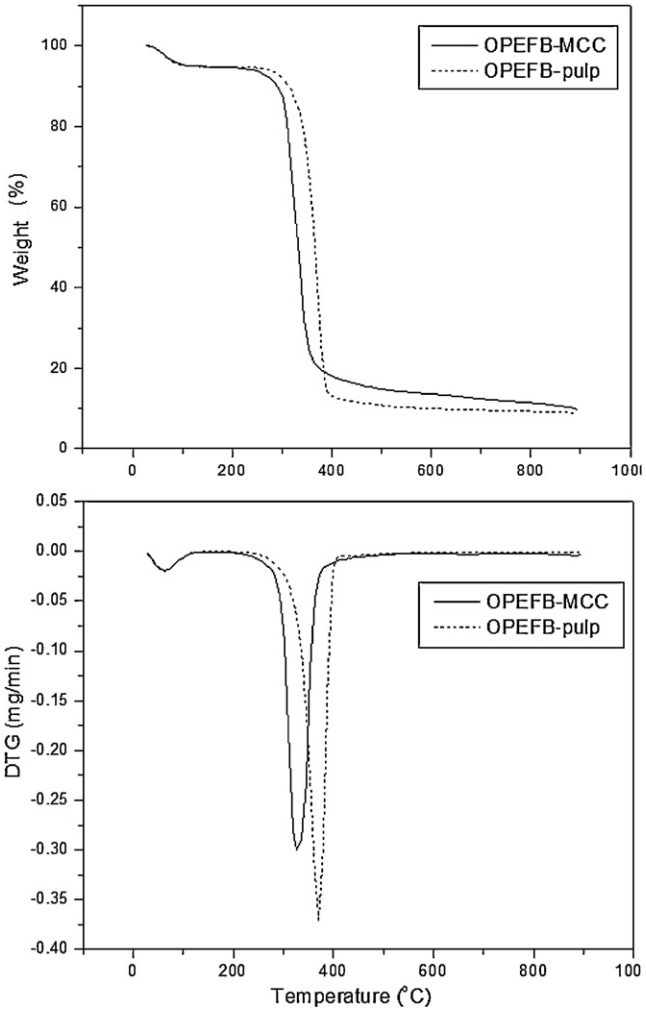

Fig. 5. Typical TGA and DTG curves for OPEFB-pulp and OPEFB-MCC.

weight loss and residual weight of OPEFB-MCC was found to be higher compare to OPEFB-pulp. The high char residue of OPEFB-MCC as compared to OPEFB-pulp is probably due to the presence of a higher amount of crystalline cellulose I which is intrinsically flame resistant (Mandal & Chakrabarty, 2011).

The decomposition peaks of OPEFB-MCC greater (326 °C) than the decomposition of MCC from jute (maximum 315 °C) as reported by Jahan et al. (2011). They reported that a decrease in the thermal stability of Jute MCC was due to the introduction of sulfate groups into the outer surface of the cellulose crystals during hydrolysis of jute cellulose. However, in this research, hydrolysis in carried out with HCl instead of H_2SO_4. Therefore, no surface sulfate group is present. Reinforcing this idea is the fact that the degradation temperatures of nanofibrils from wheat straw and soy hulls display similar degradation temperatures (Alemdar & Sain, 2008a). In view of the above results, it was concluded that the MCC sample produced from OPEFB-pulp has good thermal stability and will be suitable in the production of green biocomposites.

5. Conclusions

MCC has been successfully isolated from OPEFB-pulp, which is one of the most abundant sources of biomass planted in Malaysia. The results obtained from FT-IR analysis confirmed that chemical structure of the cellulosic fragments is not influenced by the acid hydrolysis. SEM shows that the OPEFB-MCC has a rough and compact structure, similar to C-MCC, although it exhibits much smaller fragments. AFM analysis revealed that the OPEFB-MCC obtained showed regular spherical particles. The crystallinity analysis shows that OPEFB-MCC has a high crystallinity index providing evidence that acid hydrolysis does not alter the crystal structure from the cellulose I allomorph of OPEFB-pulp. TGA analysis indicated that OPEFB-MCC produced from OPEFB-pulp has a good thermal stability. Based on these results it can be concluded that the production of OPEFB-MCC from OPEFB-pulp by acid hydrolysis is adequate for obtaining samples with high crystallinity. The prepared OPEFB-MCC has the potential to be a good reinforcing material for polymeric materials, where large surface area and good thermal properties are required.

Acknowledgments

The author M.K. Mohamad Haafiz would like to thank University Sains Malaysia (USM) and Ministry of Higher Education Malaysia (KPT) for financial support.

References

Abraham, E., Deepaa, B., Pothana, L. A., Jacobc, M., Thomasb, S., Cvelbard, U., et al. (2011). Extraction of nanocellulose fibrils from lignocellulosic fibres: A novel approach. *Carbohydrate Polymers*, *86*, 1468–1475.

Alemdar, A., & Sain, M. (2008a). Isolation and characterization of nanofibres from agricultural residues-wheat straw and soy hulls. *Bioresource Technology*, *99*, 1664–1671.

Alemdar, A., & Sain, M. (2008b). Biocomposite from wheat straw nanofibers: Morphology, thermal and mechanical properties. *Composite Science and Technology*, *68*, 557–565.

Azizi Samir, M. A. S., Alloin, F., & Dufresne, A. (2005). Review of recent research into cellulosic whiskers, their properties and their application in nanocomposite field. *Biomacromolecules*, *6*, 612–626.

Battista, O. A. (1950). Hydrolysis and crystallization of cellulose. *Industrial and Engineering Chemistry*, *42*, 502–507.

Bras, J., Hassan, M. L., Bruzesse, C., Hassan, E. A., El-Wakil, N. A., & Dufresne, A. (2010). Mechanical, barrier, and biodegradability properties of bagasse cellulose whiskers reinforced natural rubber nanocomposites. *Industrial Crops and Products*, *32*, 627–633.

Chuayjuljit, S., Su-uthai, S., & Charuchinda, S. (2010). Poly(vinyl chloride) film filled with microcrystalline cellulose prepared from cotton fabric waste: Properties and biodegradability study. *Waste Management & Research*, *28*, 109–117.

Das, K., Ray, D., Bandyopadhyay, N. R., Ghosh, T., Mohanty, A. K., & Misra, M. (2009). A study of the mechanical, thermal and morphological properties of microcrystalline cellulose particles prepared from cotton slivers using different acid concentrations. *Cellulose*, *16*, 783–793.

De Menezes, A. J., Siqueira, G., Curvelo, A. A. S., & Dufresne, A. (2009). Extrusion and characterization of functionalized cellulose whiskers reinforced polyethylene nanocomposites. *Polymer*, *50*, 4552–4563.

Eichhorn, S. J., Dufresne, A., Aranguren, M., Marcovich, N. E., Capadona, J. R., Rowan, S. J., et al. (2010). Review: Current international research into cellulose nanofibres and nanocomposites. *Journal of Material Science*, *45*, 1–33.

Eichhorn, S. J. (2011). Cellulose nanowhiskers: Promising materials for advanced applications. *Soft Matter*, *7*, 303–315.

El-Sakhawy, M., & Hassan, M. L. (2007). Physical and mechanical properties of microcrystalline cellulose prepared from agricultural residues. *Carbohydrate Polymer*, *67*, 1–10.

Fahma, F., Iwamoto, S., Hori, N., Iwata, T., & Takemura, A. (2010). Isolation, preparation, and characterization of nanofibers from oil palm empty-fruit-bunch (OPEFB). *Cellulose*, *17*, 977–985.

Fernandes, A. N., Thomas, L. H., Altaner, C. M., Callow, P., Forsyth, V. T., Apperley, D. C., et al. (2011). Nanostructure of cellulose microfibrils in spruce wood. *Proceedings of the National Academy of Sciences of the United States of America*, *108*, 1195–1203.

Goetz, L., Mathew, A., Oksman, K., Gatenholm, P., & Ragauskas, A. J. (2009). A novel nanocomposite film prepared from crosslinked cellulosic whiskers. *Carbohydrate Polymers*, *75*, 85–89.

Jahan, M. S., Saeed, A., He, Z., & Ni, Y. (2011). Jute as raw material for the preparation of microcrystalline cellulose. *Cellulose*, *18*, 451–459.

Johar, N., Ahmad, I., & Dufresne, A. (2012). Extraction, preparation and characterization of cellulose fibres and nanocrystals from rice husk. *Industrial Crops and Products*, *37*, 93–99.

Jonoobi, M., Khazaeian, A., Md Tahir, P., Azry, S. S., & Oksman, K. (2011). Characteristics of cellulose nanofibers isolated from rubberwood and empty fruit bunches of oil palm using chemo-mechanical process. *Cellulose*, *18*, 1085–1095.

Klemm, D., Heublein, B., Fink, H. P., & Bohn, A. (2005). Cellulose: Fascinating biopolymer and sustainable raw material. *Angewandte Chemie – International Edition*, *44*, 3358–3393.

Kumar, V., Maria De La, L. R. M., & Yang, D. (2002). Preparation, characterization, and tabletting properties of a new cellulose-based pharmaceutical aid. *International Journal of Pharmaceutics*, *235*, 129–140.

Lee, S-Y., Mohan, D. J., Kang In, A., Doh, G-H., Lee, S., & Han, S. O. (2009). Nanocellulose reinforced PVA composite films: Effects of acid treatment and filler loading. *Fibers and Polymers*, *10*, 77–82.

Leh, C. P., Wanrosli, W. D., Zainuddin, Z., & Tanaka, R. (2008). Optimisation of oxygen delignification in production of totally chlorine-free cellulose pulps from oil palm empty fruit bunch fibre. *Industrial Crops and Products*, *28*, 260–267.

Li, R., Fei, J., Cai, Y., Li, Y., Feng, J., & Yao, J. (2009). Cellulose whiskers extracted from mulberry: A novel biomass production. *Carbohydrate Polymers*, *76*, 94–99.

Mandal, A., & Chakrabarty, D. (2011). Isolation of nanocellulose from waste sugarcane bagasse (SCB) and its characterization. *Carbohydrate Polymers*, *86*, 1291–1299.

Mathew, A. P., Oksman, K., & Sain, M. (2006). The effect of morphology and chemical characteristics of cellulose reinforcements on the crystallinity of polylactic acid. *Journal of Applied Polymer Science*, *101*, 300–310.

Mathew, A. P., Oksman, K., & Sain, M. (2005). Mechanical properties of biodegradable composites from poly lactic acid (PLA) and microcrystalline cellulose (MCC). *Journal of Applied Polymer Science*, *97*, 2014–2025.

Nishiyama, Y. (2009). Structure and properties of the cellulose microfibril. *Journal of Wood Science*, *55*, 241–249.

Nuruddin, M., Chowdhury, A., Haque, S. A., Rahman, M., Farhad, S. F., Sarwar Jahan, M., et al. (2011). Extraction and characterization of cellulose microfibrils from agricultural wastes in an integrated biorefinery initiative. *Cellulose Chemical and Technology*, *45*, 347–354.

Petersson, L., Kvien, I., & Oksman, K. (2007). Structure and thermal properties of poly(lactic acid)/cellulose whiskers nanocomposite materials. *Composites Science and Technology*, *67*, 2535–2544.

Rånby, B. G. (1951). Cellulose and muscle – the colloidal properties of cellulose micelles. *Discussions of the Faraday Society*, *11*, 158–164 (discussion 208–213).

Rosa, S. M. L., Rehman, N., De Miranda, M. I. G., Nachtigall, S. M. B., & Bica, C. l. D. (2012). Chlorine-free extraction of cellulose from rice husk and whisker isolation. *Carbohydrate Polymers*, *87*, 1131–1138.

Rosnah, M. S., Astimar, A. B., Wan Hasamudin, W. H., & Gapor, A. M. T. (2009). Solid-state characteristics of microcrystalline cellulose from oil palm empty fruit bunch fibre. *Journal of oil palm research*, *21*, 613–620.

Satyamurthy, P., Jain, P., Balasubramanya, R. H., & Vigneshwaran, N. (2011). Preparation and characterization of cellulose nanowhiskers from cotton fibres by controlled microbial hydrolysis. *Carbohydrate Polymers*, *83*, 122–129.

Spagnola, C., Rodriguesa, F. H. A., Pereira, A. G. B., Fajardoa, A. R., Rubiraa, A. F., & Muniz, E. C. (2012). Superabsorbent hydrogel composite made of cellulose nanofibrils and chitosan–graft–poly(acrylic acid). *Carbohydrate Polymers*, *87*, 2038–2045.

Sturcova, A., Davies, G. R., & Eichhorn, S. J. (2005). Elastic modulus and stress-transfer properties of tunicate cellulose whiskers. *Biomacromolecules*, *6*, 1055–1061.

Wanrosli, W. D., Mohamad Haafiz, M. K., & Azman, S. (2011). Cellulose phosphate from oil palm biomass as potential biomaterials. *BioResource*, *6*, 1719–1740.

Wanrosli, W. D., Leh, C. P., Zainuddin, Z., & Tanaka, R. (2003). Optimization of soda pulping variable for preparation of dissolving pulps from oil palm fiber. *Holzforschung*, *57*, 106–113.

Wanrosli, W. D., Rohaizu, R., & Ghazali, A. (2011). Synthesis and characterization of cellulose phosphate from oil palm empty fruit bunches microcrystalline cellulose. *Carbohydrate Polymers*, *84*, 262–267.

Yano, H., Sugiyama, J., Nakagaito, A. N., Nogi, M., Matsuura, T., Hikita, M., et al. (2005). Optically transparent composites reinforced with networks of bacterial nanofibers. *Advanced Materials*, *17*, 153–155.